An All-Analog Sampled-Line VSWR Sensor

Grace Gomez, Devon Donahue, Robert Macfarland, Taylor Barton

*RF Power and Analog Laboratory

University of Colorado Boulder

Boulder, CO, 80309 USA

taylor.w.barton@colorado.edu

Abstract—A sampled-line reflectometer is presented that uses all-analog computation to produce a voltage proportional to the square of the load reflection coefficient, intended to be integrated into an RF front-end within an array. The novel approach for analog computation, and its dependence on sampler placement along the line is discussed. Experimental measurements of a varying load impedance are demonstrated using a microstrip line with diode samplers, operating at 3 GHz.

Index Terms—Power amplifiers, radio-frequency, reflectometry, impedance measurement, sampled-line

I. INTRODUCTION

The increasing use of arrays and electronic beamsteering techniques in communications sytems brings a new set of design challenges for the RF front-end. In particular, tightly-coupled arrays driven by size constraints are subject to scan angle dependent coupling among elements, which in turn leads to time-varying driving point impedance of the antenna. The capability to sense and adapt to this time-varying impedance, without requiring bulky magnetic-based isolators, would offer increased power amplifier (PA) reliability and performance in the RF front-end without sacrificing cost and size.

While impedence sensing and adaptation techniques have been previously presented, the majority of the prior literature employs CMOS technology [1], which offers substantial benefits in terms of on-chip digital logic at the expense of low power density. For RF applications where wide bandgap devices are needed, a multi-port reflectometry approach has been proposed that is compatible with MMIC PAs [2], but requires analog-to-digital conversion and extensive digital computation including ellipse fitting [3].

This work introduces an all-analog solution for the sampled-line reflectometer that can be used to determine the arbitrary load connected to a sampled transmission line. The proof-of-concept simplified system is based on a discrete-component design operating at 3 GHz, and calculates the square of the magnitude of the load's reflection coefficient using a simple circuit topology based on analog operational amplifiers (opamps). This preliminary result indicates that the technique could be expanded to a sampled-OMN power amplifier [3] but without the complexity of digital computation.

II. THEORY OF OPERATION

The conceptual block diagram of the analog sensor system is shown in Fig. 1, in which two power detectors are placed

This work was funded by the Air Force Office of Scientific Research (AFOSR) award number FA9550-18-1-0215.

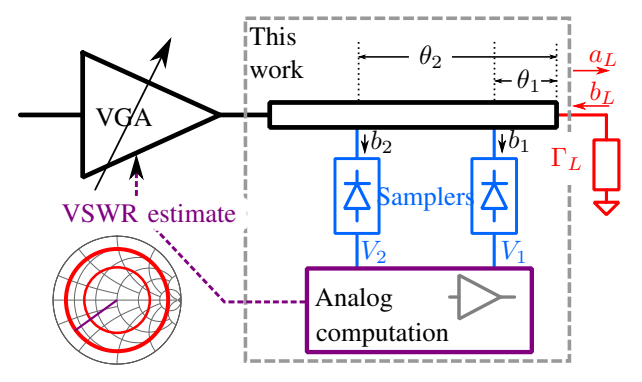


Fig. 1: Conceptual schematic of the analog impedance sensor based on a sampled-line reflectometer.

along a transmission line of characteristic impedance Z_0 that is terminated with an unknown impedance having reflection coefficient Γ_L . In the following analysis, it is assumed that the output of each power-detecting "sampler" is a voltage proportional to the square of the standing wave voltage along the transmission line, and that the samplers do not perturb the forward and reverse waves on the line. In practice, the sampler is implemented using a diode power detector with high input impedance as in [4]. We note that a minimum of three samplers is required to find the *complex*-valued load reflection coefficient; here, the objective is to find the scalar $|\Gamma_L|$ only.

Referring to Fig. 1, the output of sampler i can be related to the waves a_L and b_L at the load through the electrical length θ_i between that sampler and load as:

$$V_i = |b_i|^2 = a_L e^{-j\theta_i} + b_L e^{j\theta_i}^2$$
 (1)

using the identity $\Gamma_L = a_L/b_L$, this becomes:

$$V_i = |b_L|^2 \Gamma_L e^{-j\theta_i} + e^{j\theta_i}^2$$
 (2)

For convenience, we will initially let $b_L=1$; in other words, the incident wave is normalized (and the transmission line is assumed lossless). When this condition is not met, the outputs of both samplers will be scaled in proportion to the magnitude of the source.

If samplers 1 and 2 are, for example, located at electrical lengths $\theta_1=90^\circ$ and $\theta_2=180^\circ$ away from the load, (2) becomes

$$V_1 = |-j\Gamma_L + j|^2 \tag{3}$$

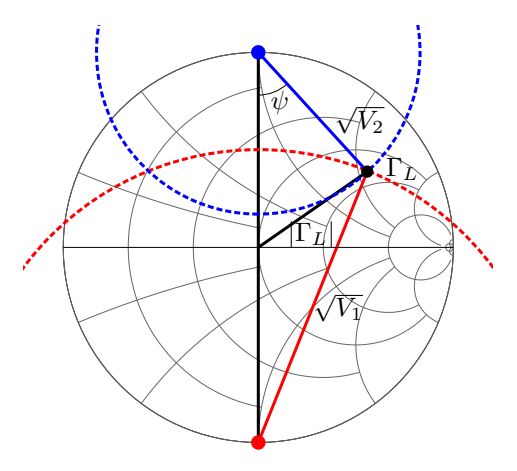


Fig. 2: Smith chart showing the analog impedance sensing concept. The circles will have centers at opposite sides of the Smith chart when the samplers are located 90° apart on the transmission line (the $\theta_1=45^{\circ}$ case is illustrated), and intersect at two points with radius $|\Gamma_L|$.

$$V_2 = |\Gamma_L + 1|^2 (4)$$

These two equations describe circles in the Γ -plane, i.e., the Smith chart, with centers at $\Gamma=1$ and $\Gamma=-1$ and radii $\sqrt{V_1}$ and $\sqrt{V_2}$, respectively. In general, if $\theta_2=\theta_1+90^\circ$, the two circle centers will be positioned 180° apart as sketched in Fig. 2 for the $\theta_1=45^\circ$ case. The load reflection coefficient, Γ_L , represents a solution to both equations, and therefore lies on one of the two circle intersection points.

We observe that two triangles are formed by the two circle center points and the point in the Γ -plane corresponding to the load impedance: one formed by $\sqrt{V_2}$, $|\Gamma_L|$, and the magnitude 1 line from the center of the Smith chart to the V_2 circle center, and a second triangle formed by $\sqrt{V_2}$, $\sqrt{V_1}$, and the Smith chart diameter (length 2). Applying the law of cosines to each triangle results in the following relations:

$$|\Gamma_L|^2 = 1 + V_2 - 2\sqrt{V_2}\cos\psi \tag{5}$$

$$V_1 = 4 + V_2 - 4\sqrt{V_2}\cos\psi \tag{6}$$

Eqns. (5) and (6) can be combined to express the reflection coefficient in terms of the two sampler outputs as:

$$|\Gamma_L|^2 = \frac{1}{2} \left(V_1 + V_2 - 2 \right)$$
 (7)

In practice, as described in Section III, the sampler output voltages $V_{1,2}$ will be scaled by some factor due to a non-unity forward wave b_L and/or the sampler behavior. A calibration to determine these scale factors, which are assumed to be constant in Γ_L , can be performed based on a straightforward characterization as described in Section III.

While (7) is valid for any phase offset between the first sampler and the load (θ_1) , we note that if $\theta_1=45^\circ$ as illustrated in Fig. 2 then the sampler outputs can be additionally used to determine whether the load impedance is capacitive $(V_2>V_1)$, resistive $(V_2=V_1)$ or inductive $(V_2< V_1)$. In other words, the

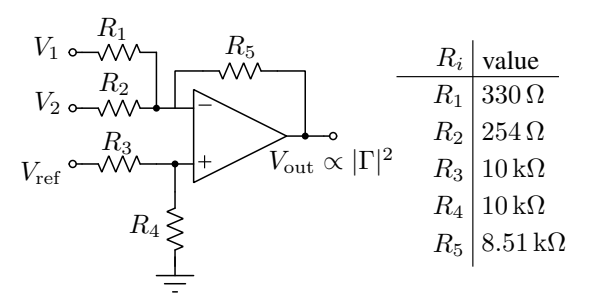


Fig. 3: Circuit schematic for the analog computation. An inverting gain configuration is used to be compatible with an analog multiplier, e.g., the AD633, which requires a negative input range.

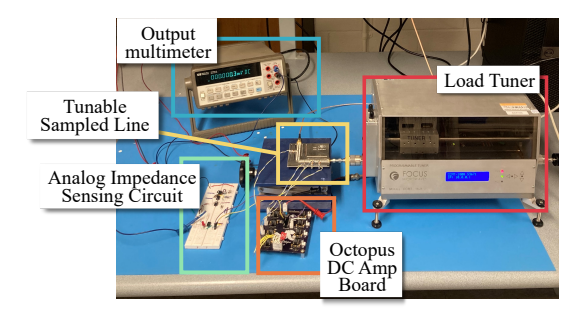


Fig. 4: Photograph of the experimental setup.

symmetry of the Γ -plane solution allows for determination of which half-plane the solution lies in if the relative magnitudes of the sampler output voltages can be compared.

III. EXPERIMENTAL VALIDATION

The computation of $|\Gamma_L|^2$ as in (7) is implemented using the op-amp circuit shown in Fig. 3. While we acknowledge that an op-amp solution is not compatible with our eventual goal of MMIC integration in a wide-bandgap process, the proof-of-concept work presented in this paper prioritizes a simple, all-analog approach that avoids digital computation. A square-root circuit, for example based on an analog multiplier within a feedback loop [5], could be added to compute $|\Gamma_L|$ from $|\Gamma_L|^2$. For a closed-loop system incorporating an optimization or analog minimization strategy, however, operating directly on $|\Gamma_L|^2$ may be preferable as it is a continuous, differentiable function [6].

The experimental testbench, shown in Fig. 4, is based on the sampled 50- Ω transmission line described in [4], terminated in a Focus Microwaves mechanical load tuner to produce the arbitrary terminating impedances. The samplers are based on Skyworks SMS7621-060 Schottky diodes, and their outputs are buffered with TC1052 chopper-stabilized op-amps. In the experimental results, the 90° separation between the samplers is set by mechanically adjusting their spacing until the standing wave nulls appear as close to 90° apart as possible. As seen in Fig. 5, the phase separation is measured to be around 87° at a 3-GHz excitation frequency.

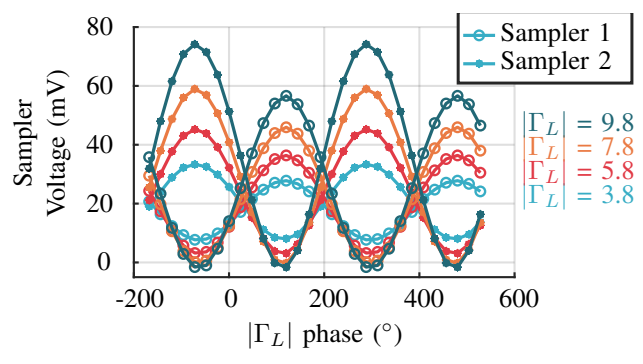


Fig. 5: Measured sampler voltages as the phase of Γ_L is swept for multiple $|\Gamma_L|$ values. The difference in sampler output voltages is attributed to slightly different coupling levels between the samplers and the microstrip line.

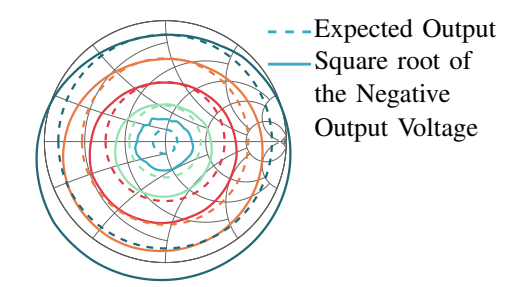


Fig. 6: Impedance measurement performed with the all-analog sensor after calibration.

In the practical system, the two sampler output voltages realistically have different scale factors even when the vector lengths [Fig. 2] are theoretically equal, e.g., for loads along the real Γ -axis. We therefore modify (7) to incorporate two scale factors, with k_0 compensating for differences in the two couplers, and k_2 for conditions where $b_L \neq 1$:

$$V_{\text{out}}(|\Gamma_L|^2) = k_0 (V_1 + k_2 V_2) - 1$$
 (8)

The two sampler output voltages are shown in Fig. 5, in which the phase of Γ_L is swept for four different $|\Gamma_L|$ values. The sampler imbalance can be observed in the different amplitudes of these standing-wave voltages, and is captured as $k_2=0.77$. For a 7 dBm input power, selected based on the desired sampler input voltage range [4], a value $k_0=25.7$ is used to produce an output voltage ranging from 0 to 1 V. These scale factor values are incorporated into the resistor selection in the op-amp circuit as summarized in Fig. 3.

An example impedance measurement at the design frequency of 3 GHz is shown in Fig. 6. For a direct comparison, the square root of the analog output voltage is computed and plotted. It can be seen that this approach produces a monotonic function in Γ_L , and has an accuracy that is likely sufficient for many RF systems. The net shift of the circles towards the bottom left of the Smith chart indicates that a more comprehensive calibration approach (or more ideally, a system with more similar sampler responses) could further improve the measurement accuracy.

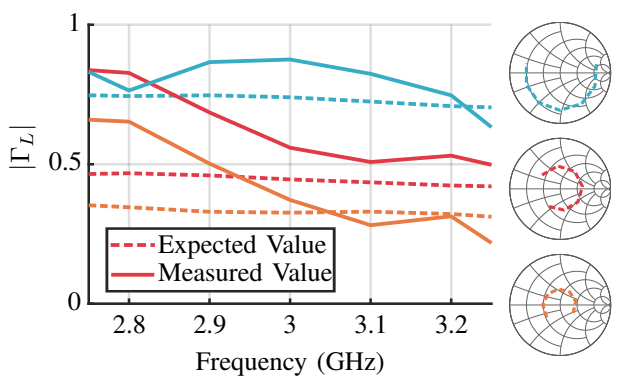


Fig. 7: Frequency performance of the impedance sensor, in which the load-pull tuner settings are held fixed at three different cases, and the expected vs. measured $|\Gamma_L|$ is displayed. At right are shown the three loading cases over the 2.7-3.3 GHz frequency range.

Fig. 7 shows the performance over frequency and various Γ_L trajectories in the Smith chart. In this experiment, the load tuner settings are held constant and the actual $|\Gamma|$ presented by the tuner over frequency is measured using a VNA. Then this VNA measurement and the analog sampler measurement are compared in terms of the magnitude of Γ_L . Successful operation over 3–3.2 GHz can be observed, with the overall function $V_{\rm out}(|\Gamma_L|)$ remaining monotonic over at least a 10% bandwidth. Extension of this technique to broader RF bandwidths is a focus of future work.

IV. CONCLUSION

The novel approach to sampled-line reflectometry presented in this work produces a voltage proportional to the square of the magnitude reflection coefficient computed by a simple analog circuit. In system scenarios where an estimate of load VSWR is sufficient for a correction scheme, this technique offers a vastly simplified approach to load computation compared to our previous work which relied on digital computation. The technique is successfully demonstrated on a 3-GHz sampled-line hardware demonstrator.

REFERENCES

- D. Nicolas, A. Serhan, A. Giry, T. Parra, and E. Mercier, "A fully-integrated SOI CMOS complex-impedance detector for matching network tuning in LTE power amplifier," in *IEEE Radio Freq. Integ. Circ. Symp.*, 2017, pp. 15–18.
- [2] D. Donahue, P. Zurek, Z. Popović, and T. Barton, "An X/Ku dual-band GaAs MMIC power amplifier with integrated load impedance sensing," in *IEEE Int. Microw. Symp.*, 2022, pp. 626–629.
- [3] D. Donahue, P. de Falco, and T. Barton, "Power amplifier with load impedance sensing incorporated into the output matching network," *IEEE Trans. Circ. Syst. I: Reg. Papers*, vol. 67, no. 12, pp. 5113–5124, 2020.
- [4] D. Donahue and T. Barton, "The w-plane as a graphical representation of sampler configuration in a sampled-network reflectometer," in ARFTG Microwave Measurement Conference, 2022, pp. 1–5.
- [5] J. Roberge, Operational Amplifiers: Theory and Practice. Wiley, 1975.
- [6] M. Pirrone, E. Dall'Anese, and T. Barton, "Zeroth-order optimization for varactor-tuned matching network," in *IEEE Int. Microw. Symp.*, 2022, pp. 502–505.